Reactions of Unsaturated Hydrocarbons at the Gold/Electrolyte Interface in Acid Solution

José L. Rodríguez and Elena Pastor*

Departamento de Química Fisica, Universidad de La Laguna, 38071 Tenerife, Spain

Volkmar M. Schmidt

Institut für Energieverfahrenstechnik, Forschungszentrum Jülich, 52425 Jülich, Germany

Received: July 26, 1996; In Final Form: March 18, 1997[⊗]

The electrochemical reactivity of ethine, ethene, and propene on polycrystalline gold in perchloric and sulfuric acid is compared. The product analysis of oxidation/reduction reactions was performed by on-line mass spectrometry and in situ FTIR spectroscopy. It was found that ethine interacts strongly with the gold/electrolyte interface, forming a chemisorbate. On the other hand, ethene and propene show a weak interaction and no adsorbed intermediates were identified after replacing the organic-containing solution by pure electrolyte. The different adsorption behavior influences the product distribution during hydrocarbon oxidation. The sole product of ethine oxidation is CO_2, whereas ethene and propene react also to partial oxidized products. The experimental results are interpreted on the basis of the electronic structures of the hydrocarbons and gold.

1. Introduction

It is well-known that gold is the most noble of all metals showing a low reactivity with respect to the interaction of the Au surface with a gaseous or liquid compound.[1] This seems to be the reason why only a few studies have been performed on the adsorption of hydrocarbons at the Au/gas interface. Auger experiments on adsorption of ethene, cyclohexene, *n*-heptene, and benzene have shown that these molecules do not adsorb on Au(111),[2] whereas these hydrocarbons chemisorb on Pt(111), forming ordered surface structures.[3−5] Even a stepped gold surface is inert to adsorption of small unsaturated hydrocarbons, and the chemisorption behavior of Au(111) and a stepped monocrystalline Au surface are indistinguishible.[2] To our knowledge, no studies on ethine adsorption on Au under ultrahigh vacuum (UHV) conditions exist in the literature.

At the Au/solution interface under electrochemical conditions small organic molecules show also rather low reactivity.[6,7] For a phenomenological classification of reactions between organics and metal electrode surfaces, several attempts have been discussed in the literature that are mainly based on experimental data.[8−11] The first group of organics is characterized by a reversible adsorption on the metal surface. Adsorbed species should have a high mobility on the surface, being easily exchanged against species in the electrolyte solution. These adsorbed species have been found to be rinsed from the surface after electrolyte exchange. The second group of species is strongly bonded to the electrode surface with or without formation of a surface chemical bond between metal and adsorbing species. This classification was proposed by Wieckowski (see ref 10) and is mainly referenced to Pt.

Another attempt has been undertaken by Lipkowski et al.[12] in order to understand the different behavior of organics in electrochemical reactions. They considered pyridine as a model substance in its interaction with Hg, Au, Ag, and Pt. The strong interaction of pyridine with Pt compared to the other metals has been rationalized on the basis of the different electronic band structures of the metals.

Recently, we have studied the reactivity of Au with respect to organics that have unsaturated carbon−carbon bonds. For C_3 alcohols it has been found that 2-propin-1-ol ($HC{\equiv}C-CH_2-OH$) exhibits a strong adsorption on polycrystalline gold whereas the corresponding alcohol with a double bond (2-propen-1-ol, $H_2C{=}CH-CH_2-OH$) shows a weak interaction.[13] To get a systematic overview on the reactivity of unsaturated species, we have studied separately ethine,[14,15] ethene,[16] and propene.[17]

The purpose of the present work is to compare the reactivity of ethine, ethene, and propene on polycrystalline gold electrodes in perchloric and sulfuric acid solution. Oxidation and reduction processes are considered and product analysis of electrochemical reactions are undertaken by means of on-line differential electrochemical mass spectrometry (DEMS) and in situ Fourier transform IR spectroscopy (FTIRS).

2. Experimental Section

Measurements were carried out in 0.05 M H_2SO_4 and 0.1 M $HClO_4$ (Merck, p.a.) electrolyte solutions prepared with Millipore-MilliQ* water. Saturated solutions of ethine (Linde), ethene (3.5, Messer-Griessheim), and propene (3.8, Messer-Griessheim) were obtained by bubbling the gas through the electrolyte solution that was previously deareated with argon (4.8, Messer-Griessheim). In the case of ethine, the gas was passed through three water traps before introducing into the electrochemical cell in order to remove traces of acetone. The purity of the ethine-containing solution was checked by gas chromatography. All experiments were made at room temperature.

DEMS studies were performed in a small flow cell directly attached to the vacuum chamber with a quadrupole mass spectrometer (Balzers QMG 412). The working electrode was a porous gold layer sputtered onto a microporous ethene−tetrafluoroethene copolymer membrane (Scimat 200/40/60, mean thickness of 60 nm, 50% porosity, mean pore diameter of 0.17 μm). The geometric area of the electrode was 0.5 cm^2 and the roughness factor varied between 5 and 6, calculated from the charge under the AuO reduction peak.[18] The counter electrode was a Au wire and the reference electrode was a reversible hydrogen electrode (RHE) in the same electrolyte solution. All

* Corresponding author.

[⊗] Abstract published in *Advance ACS Abstracts,* April 15, 1997.

S1089-5647(96)02261-4 CCC: $14.00

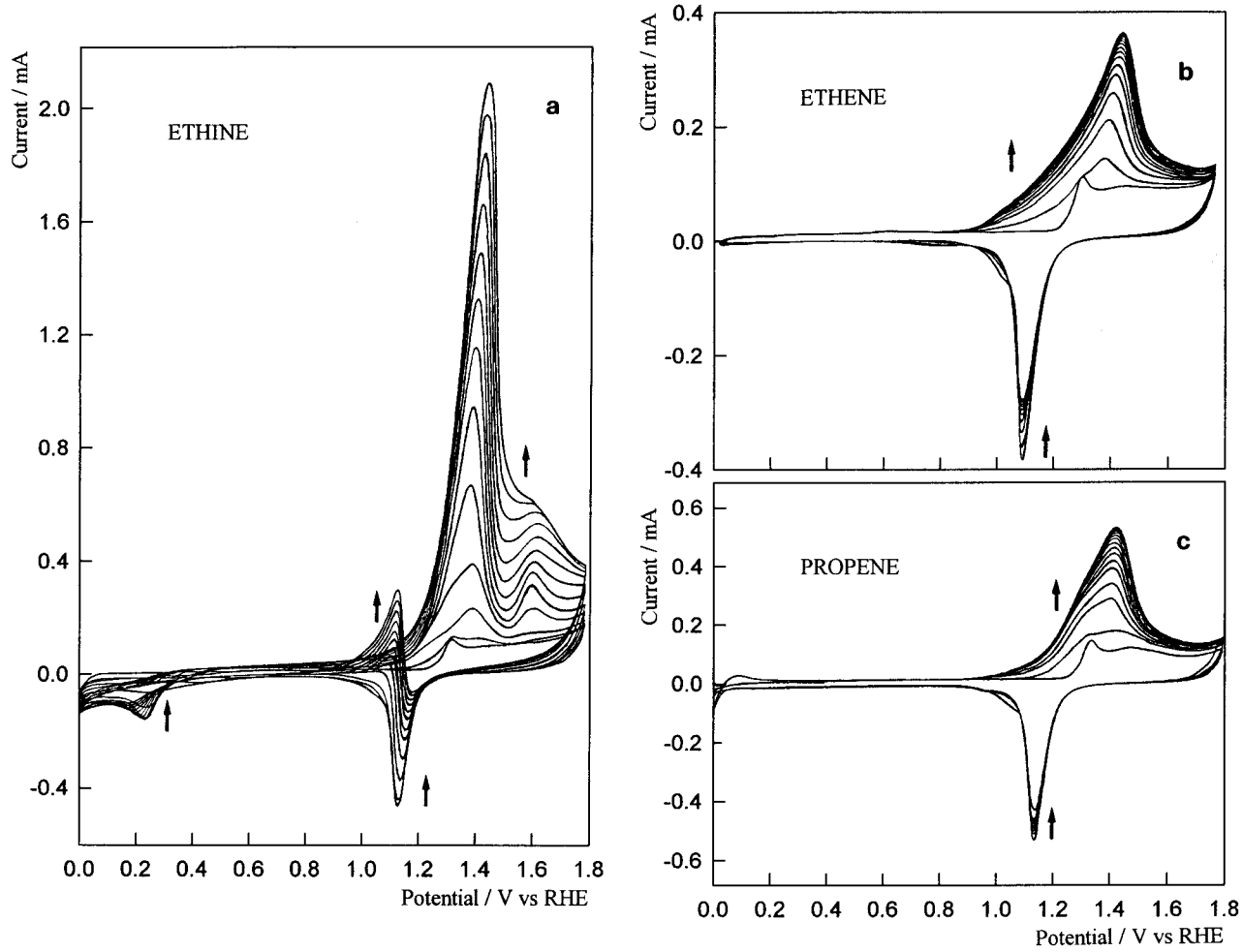

Figure 1. Succesive cyclic voltammograms for a polycrystalline Au disk during bubbling of the hydrocarbon through 0.1 M $HClO_4$ at $dU/dt = 0.10$ V s^{-1}: (a) ethine; (b) ethene; (c) propene.

potentials are given relative to this electrode. Volatile and gaseous products generated during electrochemical reactions were detected in parallel with cyclic voltamograms (CVs) by recording the ion current of the appropriate mass-to-charge (m/z) values as a function of the electrode potential, thus obtaining mass spectrometric cyclic voltamograms (MSCVs). For more experimental details on the DEMS technique see refs 19 and 20.

The FTIR spectrometer was a Digilab FTS-40 provided with a mercury−cadmium telluride (MCT) detector. The selection of p- and s-polarized light was carried out using a BaF_2-supported Al grid polarizer, and a CaF_2 window was employed. A small glass flow cell of approximately 6 mL was used. The working electrode was a polycrystalline gold disk (geometric area of 0.79 cm^2) fixed in a Teflon holder and mechanically polished to a mirror surface with diamond paste. The counter electrode was a flat Au ring and the reference was a RHE. FTIR spectra were obtained at selected potentials by applying single steps from a reference (reflectance R_0) to more positive potentials where a sample spectrum (reflectance R) was collected. Finally, spectra were calculated at each potential as the reflectance ratio R/R_0. Positive-going bands correspond to the consumption of species in the thin-layer cavity, whereas negative-going bands are associated with the production of species at the sample potential. More experimental information are described elsewhere.[21,22]

A triangular potential scan program between the onset potential for hydrogen and oxygen evolution was applied for working electrode activation in pure supporting electrolyte solution before each DEMS and FTIRS experiment.

Adsorption experiments were performed using an electrochemical flow cell combined with DEMS. For each experiment the following steps were done:[14] (i) after electrode activation, the potential was set to the adsorption potential (U_{ad}); (ii) the base electrolyte solution was replaced by the saturated solution of the corresponding unsaturated hydrocarbon at constant potential, and simultaneously, the current transient was recorded; (iii) the electrode potential was held at U_{ad} for 5 min, and then the hydrocarbon solution was exchanged by the base solution; (iv) starting from U_{ad}, positive- or negative-going potential scans were performed at $dU/dt = 0.01$ V s^{-1}. Corresponding MSCVs for appropiate m/z values were recorded simultaneously.

3. Results

3.1. Cyclic Voltammetry. Succesive cyclic voltammograms recorded at 0.10 V s^{-1} during bubbling of the hydrocarbon through 0.1 M $HClO_4$ for a polycrystalline gold disk are given in Figure 1. This electrode is used for the FTIR experiments as discussed below. In this way, the oxidation can be followed with increasing hydrocarbon concentration starting from pure electrolyte to saturated solutions (see Figure 1). For ethine (Figure 1a) three anodic current contributions are apparent in the positive-going potential scan: a shoulder at 1.22 V below the gold oxide formation and two peaks at 1.37 and 1.60 V. The anodic current increases after each potential scan by continuous bubbling of ethine, in particular the peak at 1.37 V.

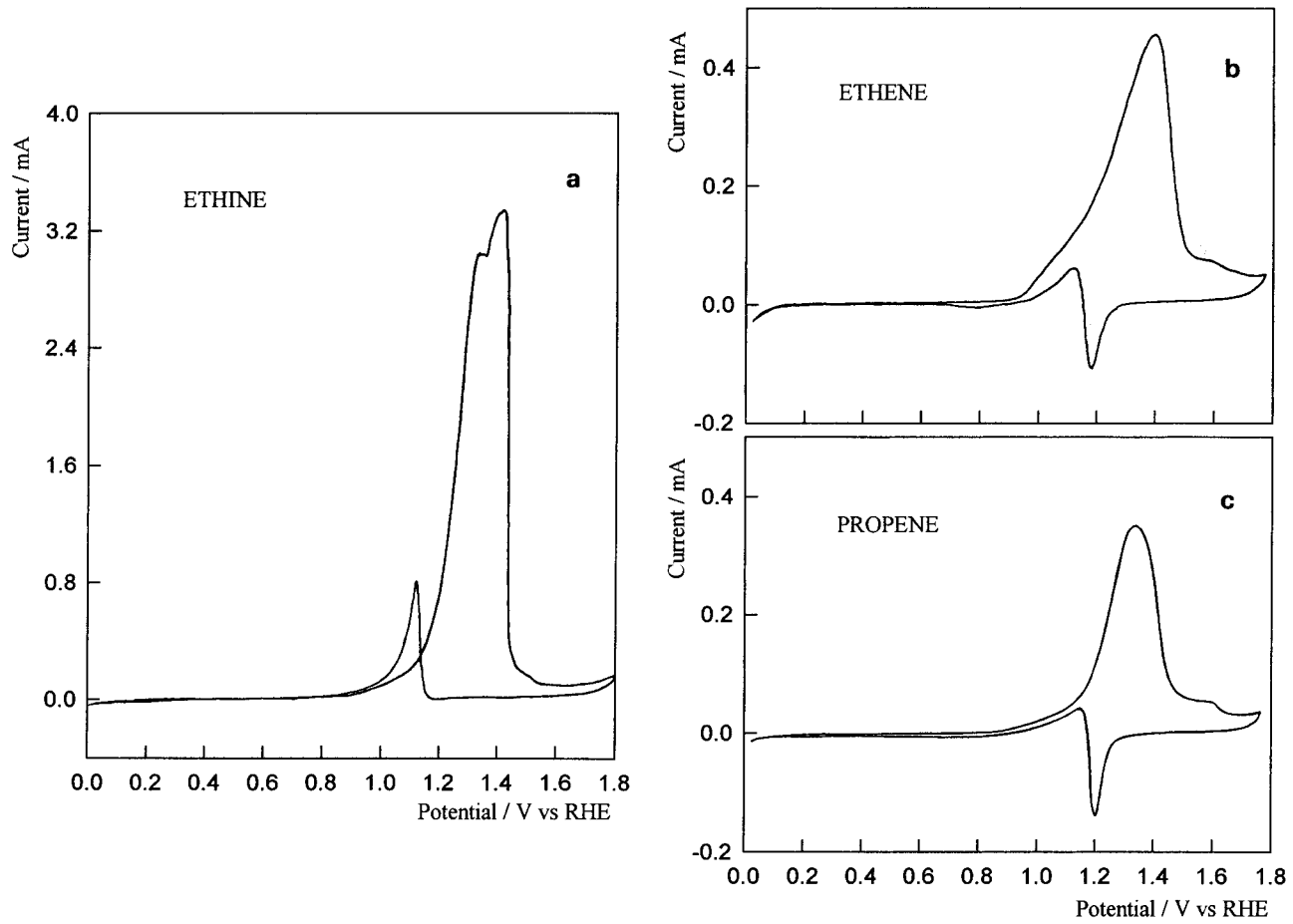

Figure 2. Cyclic voltammograms for the hydrocarbons on a porous Au electrode in 0.05 M H_2SO_4 (saturated solution) at $dU/dt = 0.01$ V s^{-1}: (a) ethine; (b) ethene; (c) propene.

In saturated solution the latter is the only well-defined peak shifted to 1.42 V. Additionally, an oxidation peak is developped at 1.13 V in the negative-going potential scan. On the other hand, a broad cathodic current peak appears at 0.24 V in the negative-going potential scans. This contribution decreases with succesive potential cycling, i.e., increasing ethine concentration.

The changes in the voltammetric profiles from low to high ethine concentrations can be explained in terms of a strong adsorption of ethine (see section 3.4). The oxidation and reduction of the chemisorbates predominate during the first cycles and should be related to the presence of the anodic contributions at 1.22 and 1.60 V in the positive-going scans and the cathodic current at 0.24 V during the reverse scans. The bulk oxidation peak occurs at 1.37 V and grows with increasing ethine concentration.

Parts b and c of Figure 1 show the CVs obtained for ethene and propene. The oxidation profiles for both gases at high concentration are similar, attaining a peak at 1.41 V. However, a difference is observed for the first five cycles. For propene two anodic current contributions can be distinguished at 1.27 and 1.42 V with similar current values, whereas for ethene only the peak at about 1.42 V is apparent, although a small anodic current can be observed below the gold oxide formation. For these hydrocarbons, the differences between the CVs for low and high concentrations are less pronounced compared with ethine, suggesting that bulk reactions of dissolved hydrocarbons are predominant over the whole concentration range.

Representatives CVs recorded at $dU/dt = 0.01$ V s^{-1} in saturated ethine, ethene, and propene solutions in 0.05 M H_2SO_4 on a porous Au electrode can be seen in Figure 2. Reproducible voltammograms were obtained when the solution was stirred slightly with the corresponding hydrocarbon between each potential cycle. The same potentiodynamic profiles were obtained on the porous Au electrode used for DEMS measurements compared to the Au disk electrode used in FTIR experiments. The electrooxidation of these compounds during the positive-going potential scan commences between 0.80 and 0.95 V (see Table 1). As shown in Figure 1, the electrooxidation of unsaturated hydrocarbons starts considerably below the onset potential of gold oxide formation (1.35 V in 0.05 M H_2SO_4 and 1.20 V in 0.1 M $HClO_4$). A comparable onset potential has been found for the oxidation of both 2-propin-1-ol and 2-propen-1-ol on gold.[13] This fact demonstrates that even in acid solutions not only gold oxide but also adsorbed H_2O and OH species are involved in the oxidation of organic molecules. Table 1 shows that the supporting electrolyte affects the threshold potential for ethene oxidation. This observation is explained by weaker perchlorate adsorption on gold compared with sulfate anions.[23] Thus, the adsorption of ethene competes with sulfate adsorption, leading to a shift of 0.10 V to more

TABLE 1: Voltammetric Data for the Oxidation of Unsaturated Hydrocarbons Recorded at $dU/dt = 0.01$ V s^{-1} on Porous Au Electrode

reactant	electrolyte	U_{onset} (V)	$U_{anodic\ peak\ I}$[a] (V)	$U_{anodic\ peak\ II}$[b] (V)
C_2H_2	0.05 M H_2SO_4	0.95	1.40	1.05
C_2H_4	0.05 M H_2SO_4	0.90	1.38	1.12
	0.1 M $HClO_4$	0.80	1.38	1.11
C_3H_6	0.05 M H_2SO_4	0.86	1.33	1.12
	0.1 M $HClO_4$	0.85	1.33	1.12

[a] In the positive-going potential scan. [b] In the negative-going potential scan.

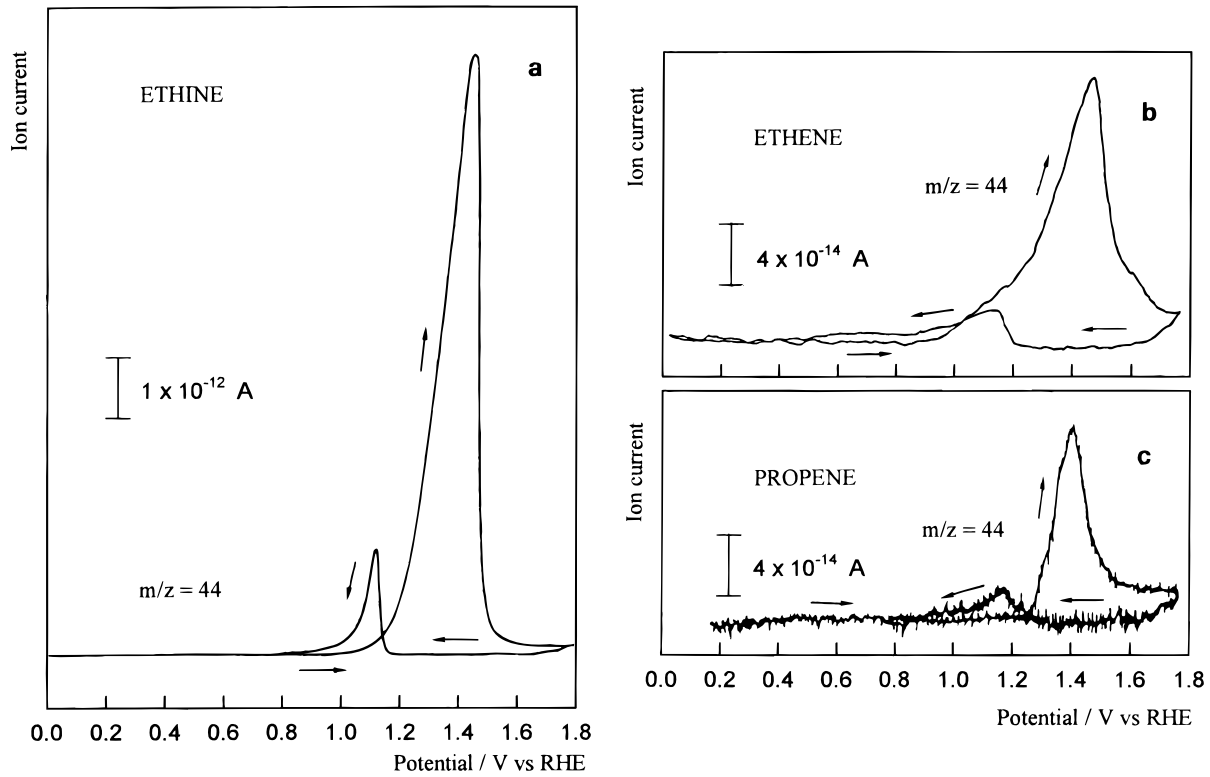

Figure 3. MSCVs for the signal $m/z = 44$ corresponding to the electrooxidation of the hydrocarbons in 0.05 M H_2SO_4 (saturated solutions) on a porous Au electrode: (a) ethine; (b) ethene; (c) propene.

positive potentials compared with perchloric acid. However, no influence of the supporting electrolyte is observed for propene. According to this interpretation, propene should adsorb more strongly than sulfate anions and propene oxidation is not affected by competing anion adsorption. Consequently, the oxidation onset potential for propene is the same in both electrolytes. Furthermore, the shift of 0.05 V to more positive potentials compared with the oxidation of ethene in perchlorate can be associated with the presence of the CH_3 group, thus stabilizing the adsorbed state of propene. On the basis of these experimental findings, the following adsorption strength sequence is suggested: ethine > propene > ethene ≈ sulfate > perchlorate.

An important difference in the voltammetric behavior of these unsaturated hydrocarbons is the fact that for the same electrode area, the oxidation current for ethine was considerably higher than the corresponding current for ethene and propene. This fact can be explained in part by the greater solubility of ethine ($c_{sat} = 5 \times 10^{-2}$ M) compared with ethene ($c_{sat} = 5.5 \times 10^{-3}$ M) and propene ($c_{sat} = 1.0 \times 10^{-2}$ M).[24] However, by comparison of the voltammetric profile for each compound, the oxidation currents are not linear with solubility. This is interpreted by different oxidation pathways involving the formation of adsorbed intermediates and will be discussed in section 4.

It should be mentioned that when the electrode in ethine-saturated solution is cycled during bubbling with ethine, the working electrode becomes brown or brownish black. This indicates the formation of a polymer layer on the electrode. In situ Raman studies have provided evidence for the formation of *trans*-polyethine.[25,26] However, this effect is not considered for further discussion.

3.2. DEMS Studies. The oxidation products formed during potential cycling were analyzed by simultaneously recording MSCVs. Figure 3 shows the corresponding mass signals for $m/z = 44$ attributed to the radical cation $[CO_2]^{\bullet+}$. This oxidation product was detected for all unsaturated hydrocarbons studied. The shape of these ion current curves is similar to the shape of the faradaic currents in the CV (Figure 2) showing CO_2 formation also in the negative-going potential scan. According to the higher electrochemical current for ethine oxidation in the CV (Figure 2a), the intensity of the ion current due to CO_2 formation is greater for ethine than for ethene and propene. No potential-dependent mass signals for alcohol and aldehyde fragments were found during the electrooxidation of ethine, thus indicating the absence of other volatile or gaseous oxidation products. However, additional potential-dependent signals appear for ethene and propene. The ion currents for $m/z = 43$ and 29 obtained for ethene and propene are shown in Figures 4 and 5, respectively. For the latter compound, the mass signal $m/z = 58$ is also given. Therefore, the oxidation of ethene and propene seems to be a more complex process than ethine oxidation.

The increase of the $m/z = 43$ and 29 signals during the positive-going potential scan at $U > 0.30$ V is associated with aldehyde fragments $[CH_3CO]^+$ and $[CHO]^+$, respectively.[27,28] Thus, for the oxidation of both C_2 and C_3 hydrocarbons, the formation of the corresponding aldehydes is expected together with the production of CO_2. According to the assignment of these signals, ethanal is formed during ethene oxidation. Therefore, the signal for $m/z = 44$ can be related to the ethanal molecular peak $[CH_3CHO]^{\bullet+}$ as well as to the molecular peak of CO_2. However, DEMS does not allow us to confirm unambiguously the formation of CO_2 in parallel with ethanal production.

A similar problem with respect to the assignment of a mass signal to different possible compounds appears regarding propene electrooxidation. The MSCV for $m/z = 58$ shown in Figure 5 could in principle be assigned to propanal (CH_3CH_2-CHO) formation and/or acetone (CH_3COCH_3). However, in this case the assignment is realized by considering the relative intensities for $m/z = 58$ and $m/z = 43$ and the fragmentation

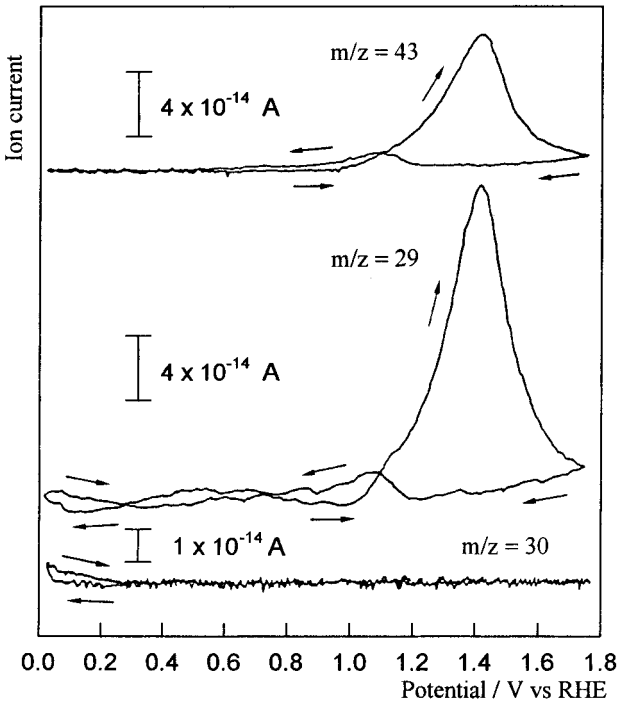

Figure 4. MSCVs corresponding to *m*/*z* values of 43, 29, and 30 for ethene in 0.05 M H_2SO_4 (saturated solution) on porous Au.

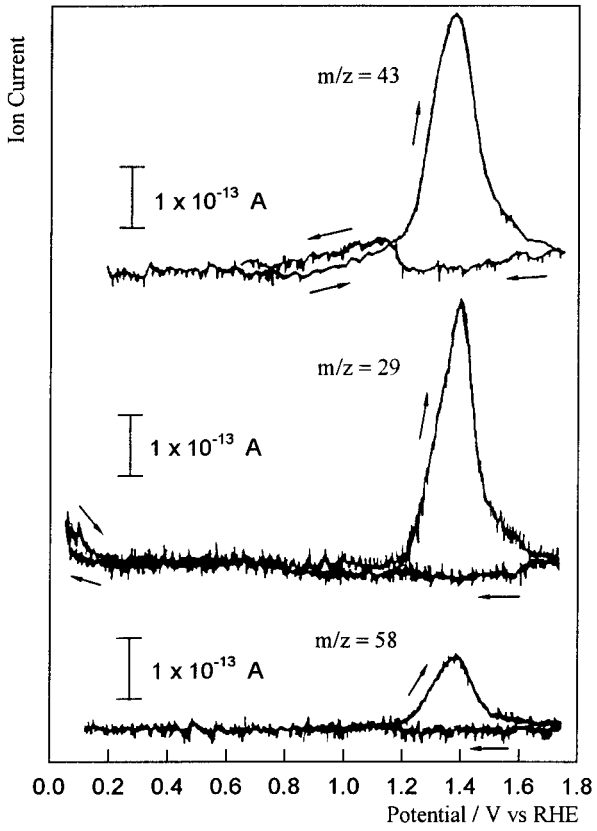

Figure 5. MSCVs corresponding to *m*/*z* values of 43, 29, and 58 for propene in 0.05 M H_2SO_4 (saturated solution) on porous Au.

probabilities expected for propanal and acetone.[27,29] The high intensity of the mass signal $m/z = 43$ implies that acetone is preferentially formed (the main peak in the mass spectra of acetone corresponds to the $[CH_3CO]^+$ fragment[27]). On the other hand, the formation of propanal should involve a small intensity for the mass signal $m/z = 43$ and a ratio of $m/z = 58$ to $m/z = 43$ of about 15, which is not the case here.

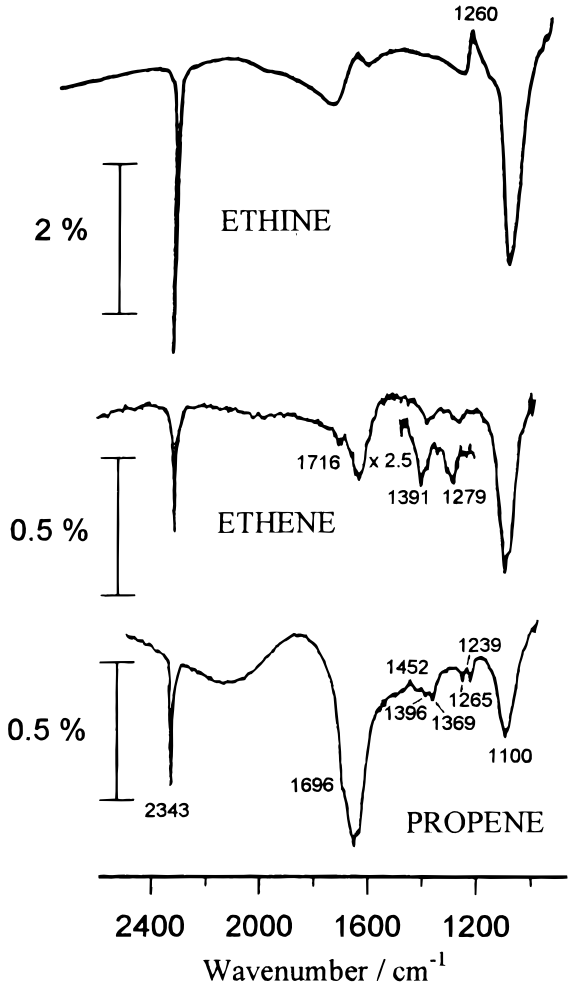

Figure 6. FTIR reflectance spectra of (a) ethine, (b) ethene, (c) propene in 0.1 M $HClO_4$ (saturated solution) on a smooth Au electrode. The sample potential was $U_{sam} = 1.15$ V for ethine and at $U_{sam} = 1.30$ V for ethene and propene. Spectra are normalized to the reference spectra collected at $U_{ref} = 0.10$ V for ethine and $U_{ref} = 0.40$ V for ethene and propene (1000 scans, resolution = 8 cm^{-1}).

The electroreduction of ethene and propene is accompanied by the increase of the ion currents for $m/z = 30$ and 29 at potentials below 0.30 V during the negative-going potential scan (Figures 4 and 5). These signals are assigned to the ethane molecular peak $[C_2H_6]^{\bullet+}$ and its fragment $[M - 1]^+$, respectively.[27]

3.3. FTIRS Studies. To verify the product distribution derived from DEMS studies, FTIR measurements were performed during electrooxidation of dissolved unsaturated hydrocarbons at different constant potentials in 0.1 M $HClO_4$. Results obtained for ethine at a sample potential $U = 1.15$ V, and ethene and propene at $U = 1.30$ V, are given in Figure 6.

All spectra show a negative band at 1100 cm^{-1}. This band is associated with the Cl−O bending mode of perchlorate ions migrating into the thin-layer cavity. The broad band around 1600−1700 cm^{-1} is due to the O−H bending mode of uncompensated water.

The problem concerning the assignment of the mass signal for CO_2 by means of DEMS during ethene and propene oxidation is solved by performing FTIR studies. The formation of CO_2 as an oxidation product from these compounds is proved by the negative band at 2343 cm^{-1} due to the C═O stretching mode of CO_2 molecules. Furthermore, FTIR spectra for dissolved ethene and propene show negative bands being associated with the formation of other oxidation products. The

TABLE 2: Oxidation Products from the Unsaturated Hydrocarbons Identified by Infrared Absorption Bands and Typical Mass Spectrometric Fragments[a]

hydrocarbon	oxidation products	IR bands (cm^{-1})	mass fragment	*m/z*
HC≡CH	CO_2	2343	$[CO_2]^{\bullet+}$	44
H_2C=CH_2	CO_2	2343	$[CO_2]^{\bullet+}$	44
	CH_3CHO		$[COH]^+$	29
			$[CH_3CO]^+$	43
	CH_3COOH	1716, 1391, 1279		
H_2C=$CHCH_3$	CO_2	2343	$[CO_2]^{\bullet+}$	44
	CH_3COCH_3	1696, 1369, 1239	$[CH_3COCH_3]^{\bullet+}$	58
			$[CH_3CO]^+$	43
	CH_3CHO		$[COH]^+$	29
			$[CH_3CO]^+$	43
	CH_3COOH	1369, 1265		

[a] For band assignment see text.

signals at 1279, 1391, and 1716 cm^{-1} for ethene and at 1265 and 1396 cm^{-1} in the case of propene are associated with the formation of acetic acid.[16,17,22] Those bands in the range 1250−1400 cm^{-1} are related to the coupled C−O stretching and O−H deformation modes of the −COOH group. The band at 1716 cm^{-1} corresponds to the C=O stretching vibration. The absence of this mode from acetic acid in the spectrum for propene is explained in terms of the superposition of the carbonyl vibration with the broad absorption band of uncompensated water centered at 1640 cm^{-1}. It is important to mention that no evidence of ethanal formation was observed in both cases. This contradiction with DEMS results can be attributed to the different experimental conditions. Taking into account the lower volatility of acetic acid (bp = 118.5 °C) compared with ethanal (bp = 20.2 °C), it would be possible that under DEMS conditions the latter is pumped into the vacuum chamber before being oxidized to acetic acid. On the other hand, the low mobility of products in the thin layer cell used for FTIR experiments leads to the accumulation of ethanal, which is oxidized further to the acid. Analogous findings have been found comparing DEMS and FTIR spectroscopy data for oxidation of *n*-propanol on Pt electrodes.[30]

The negative bands at 1239, 1369, and 1696 cm^{-1} in the spectrum obtained for propene are related to the formation of acetone as electrooxidation product.[17,28] The shoulder at 1696 cm^{-1} in the band of uncompensated water is assigned to the C=O stretching vibration of acetone. The signal at 1239 cm^{-1} may relate to the asymmetric stretching vibration of the C−C group, whereas the band at 1369 cm^{-1} should be due to the symmetric C−H deformation mode. The formation of acetone is in agreement with DEMS results in section 3.2.

The consumption of ethine is evident regarding the positive band at 1260 cm^{-1} in Figure 6.[29] It was observed that the intensity of this signal increases with positive-going potentials between 0.25 and 0.70 V, remaining constant until U = 1.20 V, whereas the stretching vibration for CO_2 at 2343 cm^{-1} increases for U > 0.80 V (not shown). This fact suggests that dissolved ethine is adsorbed on the gold surface in the range 0.25−0.80 V without being oxidized. No positive bands appear in the ethene spectra. For propene, a positive-going band associated with its consumption is observed at 1452 cm^{-1} (Figure 5). This wavenumber is interpreted as the asymmetric deformation vibration of the CH_3 group.[31,32]

Oxidation products from ethine, ethene, and propene are summarized in Table 2, together with the mass spectrometric signals for the most intense fragments and infrared vibrations assigned to these products.

3.4. Adsorption Studies. The discrimination between the electrooxidation of C_2H_2, C_2H_4, and C_3H_6 dissolved in supporting electrolyte solution and surface reactions of their adsorbed intermediates is achieved by using an electrochemical flow cell

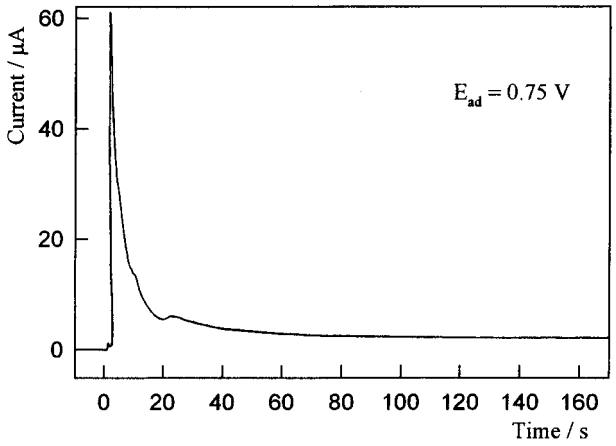

Figure 7. Current transient for ethine adsorption reaction at U_{ad} = 0.75 V on a porous Au electrode in 0.05 M H_2SO_4 saturated solution; adsorption time t_{ad} = 5 min.

in combination with DEMS. Only for ethine an anodic current transient is measured during the adsorption experiment carried out at U_{ad} between 0.20 and 0.80 V (see Figure 7 for U_{ad} = 0.75 V).[14,29] After replacement of hydrocarbon-containing solution by pure base electrolyte, a strongly bonded ethine oxidation intermediate remains on the surface. This adsorbate layer is oxidized completely in the first positive-going potential scan up to 1.75 V. In comparable experiments carried out with ethene and propene, neither anodic current in the CV nor potential-dependent ion currents were observed. This observation provides evidence for the absence of chemisorbed intermediates formed in ethene or propene adsorption. According to the classification proposed by Wieckowski,[10] these compounds show a reversible adsorption, whereas ethine interacts strongly with Au.

Figure 8a shows the voltammetric profile of adsorbed ethine oxidation intermediates in 0.05 M H_2SO_4 for the adsorption reaction at U_{ad} = 0.75 V. The oxidative electrodesorption of the adlayer commences at 0.85 V, attaining first a broad anodic current at 1.26 V followed by a second peak at 1.51 V. These contributions appear in the same potential region as those in the CVs for low ethine concentrations (see Figure 1a). This peak multiplicity gives an indication for the existence of different adsorbed intermediates that are oxidized at different potentials. The influence of the supporting electrolyte was studied by replacing H_2SO_4 by $HClO_4$. The onset potential for adsorbate oxidation is the same for both electrolytes (about 0.85−0.90 V), independent of U_{ad}. However, in sulfuric acid solution the adsorbate is mostly oxidized at potentials below the formation of gold oxide (see Figure 8a), whereas for perchloric acid the anodic current is principally apparent in the gold oxide region (not shown). This fact is due to the stronger

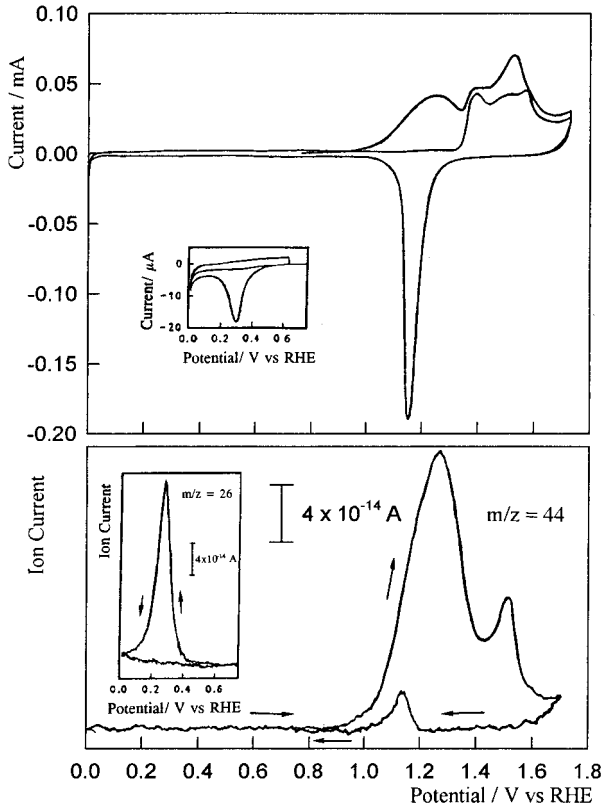

Figure 8. Electrooxidation and electroreduction of adsorbed ethine oxidation intermediates in 0.05 M H_2SO_4 on porous Au with U_{ad} = 0.75 V, t_{ad} = 5 min, and dU/dt = 0.01 V s^{-1}: (a) CVs for the oxidation and reduction (see inset) of the adsorbates, where first and second potential cycles are shown; (b) corresponding MSCVs for m/z = 44 and 26 (see inset) for adsorbates oxidation and reduction, respectively. Only the first cycle after adsorption is shown.

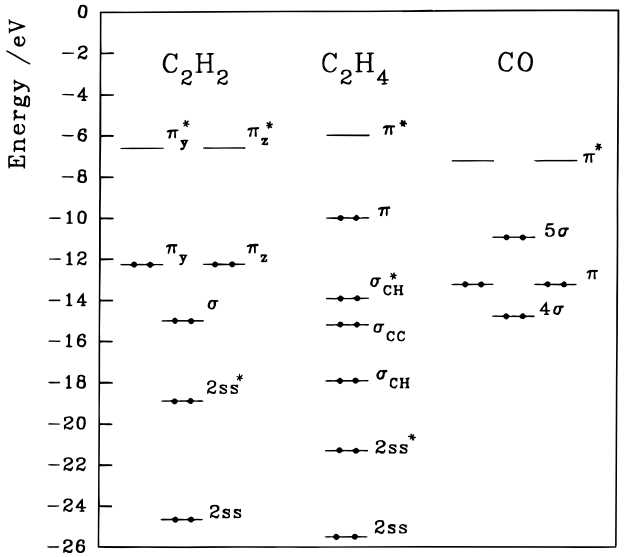

Figure 9. Energy level correlation diagrams for ethine, ethene, and CO. The zero of the energetic scale corresponds to the position of the vacuum level.

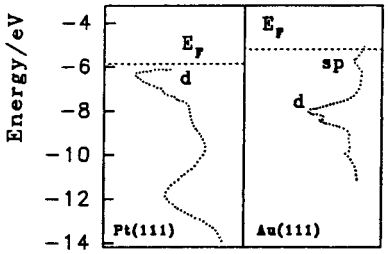

Figure 10. Density of states for Pt(111) and Au(111). The dashed line indicates the position of the Fermi level for each metal. The zero of the energy scale corresponds to the position of the vacuum level.

adsorption of HSO_4^-/SO_4^{2-} visible by the positive shift of 0.10 V for gold oxide formation compared to perchloric acid.[23] The complete oxidation of the adsorbate from ethine occurs in one potential cycle. The second potential scan corresponds to a typical CV in supporting electrolyte. The simultaneously recorded MSCV for m/z = 44 (Figure 8b) shows the same potential-dependent features similar to those of the anodic current in the voltammetric profile. In the reverse scan, as soon as the Au surface becomes free from oxide, a small CO_2 signal is obtained at 1.15 V. No products other than CO_2 were detected by mass spectrometry during adsorbate oxidation.

The inset of Figure 8a shows the CV for the reductive electrodesorption of the adsorbed ethine oxidation intermediate formed at the same U_{ad} (0.75 V). In the first negative-going potential scan, a reduction peak is present at 0.28 V. This peak accords with the voltammetric feature apparent in Figure 1a during the reverse scan in the same potential region. Potential-dependent mass signals appear for m/z = 26 and 28. The former corresponds to the sharp peak given in the inset of Figure 8b and it is assigned to the molecular peak $[C_2H_2]^{\bullet+}$ of ethine.[27] The signal for m/z = 28 (not shown) is much smaller and corresponds to $[C_2H_4]^{\bullet+}$ related to the formation of ethene. This fact is explained by a hydrogenation reaction of the adsorbate[13] with the small amount of hydrogen adatoms present on the surface of a potential cycled gold electrode.[33]

The reductive electrodesorption of the adsorbate is not complete during the first negative-going potential scan down to 0 V. About 10% of the adsorbate remain on the surface after the first reduction cycle. The same CV and MSCV profiles for adsorbate reduction are observed in perchloric acid. From isotope-labeling studies, $(C_2H)_{ad}$ and $C_2)_{ad}$ have been proposed as adsorbate species formed during oxidative ethine adsorption.[15]

4. Discussion

The experimental results obtained by CV in combination with DEMS and FTIRS evidently show that the interaction of an unsaturated hydrocarbon with the gold/electrolyte interface affects significantly the product distribution during electrooxidation. Therefore, adsorption of ethine, ethene, and propene is considered as the first step in the oxidation reaction pathway. One approach to interpretate the experimental results is to look at the electronic structure of the hydrocarbons and their bonding modes to the surface. Figure 9 shows the energy level correlation diagrams for ethine[34] and ethene.[35] For comparison the corresponding diagram for CO[36] is also given. These molecules exhibit unoccupied π^* orbitals. The nature of the surface chemical bond between CO and a transition metal such as Pt (see the energy diagram of Pt(111) in Figure 10) is well understood:[37,38] the population of 5σ orbitals of the carbon monoxide due to the chemisorption is reduced and that of the antibonding $2\pi^*$ is increased (back-donation). However, through a series of transition metals, it has been observed that the population of the 5σ level in chemisorbed CO is almost constant and the population of $2\pi^*$ rises significantly.[39] Therefore, the back-donation interaction is predominant and the capacity of the metal to donate to $2\pi^*$ CO orbital mainly accounts for CO surface chemical bond.

In a similar way, the Dewar−Chatt−Duncanson model (π−d bonding) was established for the adsorption of unsaturated

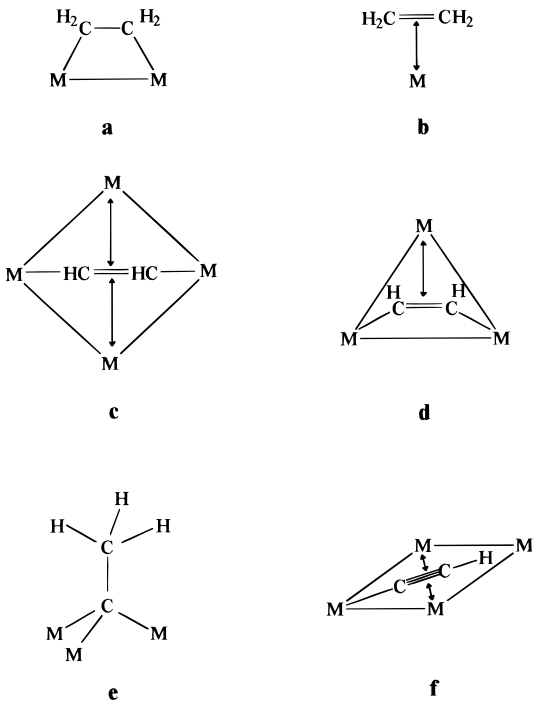

Figure 11. Possible structures for adsorbates of ethene (a, b, and e) and ethine (c−f). The arrows denote a π interaction.

hydrocarbons on transition metals.[35,40] The π−d interactions in transition metal/unsaturated hydrocarbon complexes consist of two contributions: the donation of electron density from the π bond of the alkene or alkine to the unoccupied d orbitals of the metal; the back-donation of electron density from the d orbitals of the metal to the empty π* antibonding orbitals in the hydrocarbon.[41] It has been proposed that surface coordination involves bonding similar to those found in complexes of transition metals/unsaturated hydrocarbon, since similar experimental findings have been observed in both cases.[35]

EELS (electron energy loss spectroscopy) spectra for ethine and ethene adsorbed on transition metals single-crystal surfaces have revealed the occurrence of certain patterns in the spectra that can be assigned to particular structures of the adsorbed species.[42] Ethene at low temperatures (<250 K) adsorbs as $(C_2H_4)M_n$ (M = metal, $n = 1$ or 2), where n denotes the number of metal surface atoms involved in the adsorption. In general, two chemisorbed species can be distinguished: di-σ adsorbed (Figure 11a) and π adsorbed (Figure 11b) ethene.[42] For ethine adsorbed at low temperatures a carbon−carbon bond order between 2 and 1 has been obtained. These large changes in bond order are due to the interaction of the C_2H_2 chain with four (Figure 11c) or three (Figure 11d) surface atoms rather than two or one as in the ethene case.[42] At room temperatures, adsorbates from ethene and ethine are denoted as $(C_2H_x)M_n$ (n = 2 or 3).[42−44] In this case, C−H bonds of the adsorbed species from ethene and ethine are broken and the species resulting from these processes is usually the ethylidyne, CH_3CM_3 (Figure 11e), which adsorbs in 3-fold triangular sites.[42−44] Finally, a model for the C≡CH species is proposed with the triple bond almost parallel to the surface (Figure 11f).[45]

Figure 10 shows the energies of the electronic bands for Pt and Au[12] plotted on a common energy scale (the dashed line locates the Fermi level (E_F) for each metal). First, it has to be considered that for symmetry reasons the π orbitals of C_2H_2 and C_2H_4 can only mix with d and $p_{x,y}$ electronic states in the metal.[12,46,47] For Pt the Fermi level is located in the d band. By comparison of the energies of Pt electronic band in Figure 10 with the energy of the molecular orbitals for ethine and ethene in Figure 9, it is evident that the π levels of C_2H_2 and C_2H_4 can form a strong σ bond involving the partially occupied d electronic states of the metal. These metal states can also mix with the π* orbitals of the hydrocarbons, reinforcing the chemisorption bond through back-donation. In contrast, for Au the filled d band is located 2 eV below E_F. The π* orbitals from the hydrocarbons lie above the d band but below E_F in a low density of states region occupied by s and p electrons.[35] Thus, electron density from the alkene π orbital can be donated to the half-filled s orbital in this metal, since the d−s promotion energies are quite small.[48] The work function value locating E_F of the metal is 5.22 eV for polycrystalline Au, and this value is similar to that for Au(111) given in Figure 11 (5.26 eV).[49]

The electrochemical results indicate that the adsorption of ethene and propene on polycrystalline Au electrodes is reversible and that adsorbed species are rinsed from the electrode by the pure supporting electrolyte. A comparable behavior has been reported for 2-propen-1-ol.[13] No IR bands related to adsorbates appear with ethene and propene in the solution (Figure 6). This is explained by a flat orientation with the C═C bond parallel to the surface. According to the surface selection rule for IR spectroscopy,[6] the C═C and ═C−H vibrations cannot be detected. Thus, ethene and propene interact with the surface with the intact π system as sketched in Figure 11b. In this case, no rehybridization should be observed. This conclusion is confirmed by SERS studies on the adsorption of alkenes at gold electrodes.[25,50]

Ethine has two π bonds for the interaction with Au. Compared with the electronic structure of ethene in Figure 9, ethine should adsorb more strongly. This interpretation fits well with the experimental finding that the adsorption of ethine is irreversible and that adsorbed ethine intermediates are stable in ethine-free electrolyte solution. As in the case of ethene, no vibration modes corresponding to the C≡C and ≡C−H groups for adsorbed ethine are observed in the FTIR spectra. The triple bond of ethine can be broken, leading to the formation of a σ bond with the metal accompanied with sp^2 rehybridization. Possible structures are sketched in parts c and d of Figure 11. However, the absence of ≡C−H vibration modes could indicate an orientation parallel to the gold surface. Another explanation is the break of at least one ≡C−H bond and the formation of acetylidic species (for example, C_2H) in which the C≡C bond is intact (see Figure 11f). This interpretation is supported by the adsorption experiments (see section 3.4). The anodic current transients for $U_{ad} = 0.20-0.80$ V are not accompanied by CO_2 formation, which can be confirmed by the absence of any ion current signal for $m/z = 44$ in this potential range (compare with Figure 3a). The charge density of about 200 μC/cm^2 involved in the transient (see Figure 7) is also too large to be assigned only to a change in the double-layer capacity.[51] Thus, the anodic transient observed during ethine adsorption is explained by the release of protons and electrons from C_2H_2. The adsorbed intermediate being formed has a higher oxidation state than the original ethine molecule. In a previous work using isotope-labeling, adsorbed intermediates such as C_2 and C_2H have been proposed.[15] Moreover, the calculation of the charge densities involved during ethine adsorption and the complete oxidation of adsorbed intermediates to CO_2 on Au single crystals have shown that the adsorbate requires four surface sites independent of the crystal orientation.[51] These results agree with the structures proposed in parts c and f of Figure 11. In this respect it is interesting to mention that these species were also found for ethine adsorption on an oxygen-covered Ag(110) surface at 100 and 280 K.[45] According to this analogy, the electrochemical environment seems to have similar properties

as an oxygen layer under UHV conditions. Both situations favor the dissociative adsorption of ethine.

SERS spectra in the literature for different alkines have shown that the ν(C≡C) band appears in the same frequency region for all compounds investigated.[26] This observation suggests the formation of surface $\sigma\pi$ bonds, which require triple bonds to lie flat on the metal. The absence of detectable ≡C−H stretching bands for ethine and 1-alkynes supports the formation of acetylidic surface bonds.[26] Besides the ν(C≡C) vibration, all adsorbates exhibit a broad band in the C=C bond region, thus indicating that the adsorbed alkynes exist in several states of hybridization.[26] These experimental facts agree well with the interpretation given in the present paper.

The oxidation of the adsorbed intermediates occurs in a second step for all the hydrocarbons studied (Figures 1 and 2), yielding the products summarized in Table 2. From the analysis of these compounds, the reaction paths are proposed for each hydrocarbon molecule. For ethene and propene, the electrooxidation occurs after the reversible adsorption (eq 1), in two different pathways simultaneously. The first one produces CO_2 as a final product (eq 2), and the second involves the formation of partially oxidized compounds (eq 3). For the latter, the addition of water to the carbon−carbon double bond seems to determine the oxidation product. Accordingly, the following reactions can be written:

$$\mathrm{Au} + \mathrm{H_2C{=}CHR} \rightarrow \mathrm{Au[H_2C{=}CHR]_{ads}} \quad (1)$$

$$\mathrm{Au[H_2C{=}CHR]_{ads}} + n(\mathrm{H_2O})\mathrm{Au} \rightarrow \mathrm{Au} + n'\mathrm{CO_2} + x\mathrm{H^+} + x\mathrm{e^-} \quad (2)$$

$$\mathrm{Au[H_2C{=}CHR]_{ads}} + (\mathrm{H_2O})\mathrm{Au} \rightarrow \mathrm{Au} + \mathrm{CH_3COR} + 2\mathrm{H^+} + 2\mathrm{e^-} \quad (3)$$

where R = H for ethene and R = CH_3 for propene. In these equations "Au" denotes the metal surface without considering the number of gold sites involved in the reaction. Thus, eq 3 describes the formation of ethanal from ethene and acetone from propene. Ethanal can further react with water on the Au surface, forming acetic acid:

$$\mathrm{CH_3CHO} + (\mathrm{H_2O})\mathrm{Au} \rightarrow \mathrm{Au} + \mathrm{CH_3COOH} + 2\mathrm{H^+} + 2\mathrm{e^-} \quad (4)$$

Since ethanal is also detected from propene, a third reaction pathway should be considered for propene electrooxidation, which is the fragmentation of the molecule upon adsorption:

$$\mathrm{H_2C{=}CH{-}CH_3} + 2(\mathrm{H_2O})\mathrm{Au} \rightarrow \mathrm{Au[H_2C{=}CH]_{ads}} + \mathrm{CO_2} + 7\mathrm{H^+} + 7\mathrm{e^-} \quad (5)$$

The adsorbed species formed in eq 5 is comparable to that for ethene in eq 1 and electrooxidizes easily to ethanal according to eq 3 and to acetic acid according to eq 4.

The formation of ethane from ethene and propene is explained by a reaction of hydrogen with $Au[CH_2{=}CH_2]_{ads}$ and $Au[CH_2{=}CH]_{ads}$, respectively:

$$\mathrm{Au[H_2C{=}CH_2]_{ads}} + 2(\mathrm{H})\mathrm{Au} \rightarrow \mathrm{Au} + \mathrm{CH_3CH_3} \quad (6a)$$

$$\mathrm{Au[H_2C{=}CH]_{ads}} + 3(\mathrm{H})\mathrm{Au} \rightarrow \mathrm{Au} + \mathrm{CH_3CH_3} \quad (6b)$$

On the other hand, ethine adsorbs irreversibly on gold, producing a mixed layer of different residues:

$$\mathrm{Au} + \mathrm{HC{\equiv}CR} \rightarrow \mathrm{Au[intermediates]_{ads}} \quad (7)$$

where R = H for ethine. These intermediates oxidize only to CO_2:

$$\mathrm{Au[intermediates]_{ads}} + n(\mathrm{H_2O})\mathrm{Au} \rightarrow \mathrm{Au} + n'\mathrm{CO_2} + x\mathrm{H^+} + x\mathrm{e^-} \quad (8)$$

This difference in the reactivity between compounds with a triple bond and molecules having a double bond has been observed in the case of 2-propin-1-ol ($HC{\equiv}C{-}CH_2OH$) and 2-propen-1-ol ($H_2C{=}CH{-}CH_2OH$).[13] For ethene and propene, a reversible adsorption has been observed for 2-propen-1-ol that corresponds to eq 1, whereas an irreversible interaction was found for 2-propin-1-ol in agreement with eq 7, both for R = CH_2OH. Also, CO_2 appears as an oxidation product following reactions 2 and 8.

5. Conclusions

The reactivity of ethene, propene, and ethine in acid solution on a polycrystalline Au electrode is comparatively studied. DEMS and FTIRS are used as spectroelectrochemical techniques in order to elucidate reaction products.

It is demonstrated that the first step for the oxidation/reduction reaction pathways of these molecules is the adsorption at the electrode surface. The interaction with the gold/electrolyte interphase for ethene and propylene is characterized by a reversible adsorption, and adsorbed species are not stable in the electrolyte solution. In contrast to results reported in the literature for the metal/gas interface under UHV conditions showing no adsorption of unsaturated hydrocarbons at room-temperature occurring for group IB metals, ethine exhibits a strong interaction with Au, leading to the formation of chemisorbed intermediates. The differences found for compounds with double and triple bonds with respect to adsorption followed by oxidation/reduction reactions are explained by the electronic structure of the hydrocarbons and Au.

Ethine oxidizes only to CO_2 because of the formation of irreversible adsorbed species that facilitate the fragmentation of the carbon−carbon bond. In the case of ethene and propene, partially oxidized products are obtained, and ethane is detected as the sole reduction product.

Previous studies with unsaturated C_3 alcohols corroborate the experimental findings obtained for unsaturated hydrocarbons. Thus, it can be predicted that organic molecules with a carbon−carbon triple bond (ethine and 2-propin-1-ol) adsorb strongly on Au electrodes in acid media accompanied by the formation of chemisorbates. For molecules with a double bond (ethene, propene, 2-propen-1-ol), a reversible interaction is expected.

References and Notes

(1) Hammer, B.; Nerskov, J. K.; *Nature* **1995**, *376*, 238.
(2) Chesters, M. A.; Somorjai, G. A. *Surf. Sci.* **1975**, *52*, 21.
(3) Morgan, A. E.; Somorjai, G. A. *J. Chem. Phys.* **1969**, *51*, 3309.
(4) Gland, J. L.; Somorjai, G. A. *Surf. Sci.* **1973**, *38*, 157.
(5) Gland, J. L.; Baron, K.; Somorjai, G. A. *J. Catal.* **1975**, *36*, 305.
(6) Lipkowski, J., Ross, P. N., Eds. *Adsorption of Molecules at Metal Electrodes*; VCH: Weinheim, 1992.
(7) Lipkowski, J., Ross, P. N., Eds. *Structure of Electrified Interfaces*; VCH: Weinheim, 1993.
(8) Horanyi, G. *J. Electroanal. Chem.* **1974,** *51*, 163.
(9) Wieckowski, A. *Electrochim. Acta* **1981,** *26*, 1121.
(10) Wieckowski, A. In *Modern Aspects of Electrochemistry*; White, R. E., Bockris, J. O'M, Conway, B. E., Eds.; Plenum Press: New York, London, 1991; Vol. 21, p 64.
(11) Michelhaugh, S. L.; Bhardwaj, C.; Cali, G. J.; Bravo, B. G.; Bothwell, M. E.; Berry, G. M.; Soriaga, M. P. *Corrosion* **1991,** *95*, 7771.
(12) Lipkowski, J.; Stolberg, L.; Yang, D.-F.; Pettinger, B.; Mirwald, S.; Henglein, F.; Kolb, D. M. *Electrochim. Acta* **1994,** *39*, 1045.
(13) Pastor, E.; Schmidt, V. M.; Iwasita, T.; Arévalo, M. C.; González, S.; Arvia, A. J. *Electrochim. Acta* **1993**, *38*, 1337.

(14) Schmidt, V. M.; Pastor, E. *J. Electroanal. Chem.* **1994,** *369*, 271.
(15) Schmidt, V. M.; Pastor, E. *J. Phys. Chem.* **1995**, *99*, 13247.
(16) Pastor, E.; Schmidt, V. M. *J. Electroanal. Chem.* **1995,** *383*, 175.
(17) Schmidt, V. M.; Pastor, E. *J. Electroanal. Chem.* **1996,** *401*, 155.
(18) Angerstein-Kozlowska, H.; Conway, B. E.; Hamelin, A.; Stoicoviciu, L. *Electrochim. Acta* **1986**, *31*, 1951.
(19) Wolter, O.; Heitbaum, J. *Ber. Bunsen-Ges. Phys. Chem.* **1984**, *88*, 2.
(20) Bittins-Cattaneo, B.; Cattaneo, E.; Königshoven, P. Vielstich, W. In *Electroanalytical Chemistry: A Series of Advances*; Bard, A., Ed.; Marcel Dekker: New York, 1991; Vol. 17, p 181
(21) Nart, F. C.; Iwasita, T. *Ber. Bunsen-Ges. Phys. Chem.* **1990**, *94*, 1030.
(22) Iwasita, T.; Rasch, B.; Cattaneo, E.; Vielstich, W. *Electrochim. Acta* **1989**, *34*, 1073.
(23) Borkowska, Z.; Stimming, U. *J. Electroanal. Chem.* **1991**, *312*, 209.
(24) Stephen, H., Stephen, T., Eds. *Solubilities of Inorganic and Organic Species*; Pergamon Press: Oxford, 1963; Vol. 1.
(25) Patterson, M. L.; Weaver, M. J. *J. Phys. Chem.* **1985**, *89*, 5046.
(26) Feilchenfeld, H.; Weaver, M. J. *J. Phys. Chem.* **1989**, *93*, 4276.
(27) Stenhagen, E., Abrahamsson, S., McLafferty, F. W., Eds. *Atlas of Mass Spectral Data*; Interscience: New York, 1969.
(28) Hesse, M.; Meier, M.; Zeeh, B. In *Spektroskopische Methoden in der organischen Chemie*; Thieme Verlag: Stuttgart, 1984.
(29) Schmidt, V. M.; Pastor, E. *J. Electroanal. Chem.* **1994,** *376*, 65.
(30) Pastor, E.; Wasmus, S.; Iwasita, T.; Arévalo, M. C.; González, S.; Arvia, A. J. *J. Electroanal. Chem.* **1993**, *350*, 97.
(31) Socrates, G. In *Infrared Characteristic Group Frequencies*; Wiley: New York, 1980.
(32) Ransley, I. A.; Ilharco, L. M.; Bateman, J. E.; Sakakini, B. H.; Vickerman, J. C.; Chesters, M. A. *Surf. Sci.* **1993**, *298*, 187.
(33) Martins, M. E.; Podestá, J. J.; Arvia, A. J. *Electrochim. Acta* **1987**, *32*, 1013.
(34) Anderson, A. B.; Mehandru, S. P. *Surf. Sci.* **1984**, *136*, 398.
(35) Felter, T. E.; Weinberg, W. H. *Surf. Sci.* **1981**, *103*, 265.
(36) Shiller, P.; Anderson, A. B. *J. Electroanal. Chem.* **1992**, *339*, 201.
(37) Fleischmann, M.; Thrisk, H. R.; Delahay, P. In *Advances in Electrochemistry and Electrochemical Engineering*; Interscience: New York, 1969; Vol. 3, p 123.
(38) Ishi, S.; Ohno, Y.; Viswanathan, B. *Surf. Sci.* **1985**, *161*, 349.
(39) Sung, S.; Hoffmann, R. *J. Am. Chem. Soc.* **1985**, *107*, 578.
(40) Demuth, J. E. *IBM J. Res. Dev.* **1978**, *22*, 265.
(41) Duddel, D. A. In *Spectroscopic and Structure of Molecular Complexes*; Yarnwood, J., Ed.; Plenum Press: New York, 1973; p 427.
(42) Sheppard, N. *J. Electron. Spectrosc. Relat. Phenom.* **1986**, *164*, 167.
(43) Demuth, J. E. *Surf. Sci.* **1979**, *80*, 367.
(44) Kesmodel, L. L.; Dubois, L. H.; Somorjai, G. A. *J. Chem. Phys.* **1979**, *70*, 2180.
(45) Stuve, E. M.; Madix, R. J.; Sexton, B. A. *Surf. Sci.* **1982**, *123*, 491.
(46) Woodward, R. B.; Hoffmann, R. *J. Am. Chem. Soc.* **1965**, *87*, 395.
(47) Hubbard, A. T.; Young, M. A.; Schoeffel, J. A. *J. Electroanal. Chem.* **1980**, *114*, 273.
(48) Bradshaw, A. M.; Pritchard, J. J. *Proc. R. Soc. London, Ser. A* **1970**, *316*, 169.
(49) Hansson, G. V.; Flodstron, S. A. *Phys. Rev. B* **1978**, *18*, 1572.
(50) Patterson, M. L.; Weaver, M. J. *J. Phys. Chem.* **1985**, *89*, 1331.
(51) Schmidt, V. M.; Stumper, J.; Schmidberger, J.; Pastor, E.; Hamelin, A. *Surf. Sci.* **1995**, *335*, 197.